INTERNATIONAL JOURNAL OF SATELLITE COMMUNICATIONS AND NETWORKING
Int. J. Satell. Commun. Network. 2007; **25**:147–165
Published online in Wiley InterScience (www.interscience.wiley.com). DOI: 10.1002/sat.869

Ka-band link optimization with rate adaptation for Mars and lunar communications

Jun Sun[1,*,†], Jay Gao[2], Shervin Shambayati[2] and Eytan Modiano[1]

[1] *Massachusetts Institute of Technology, Cambridge, MA 02139, U.S.A.*
[2] *Jet Propulsion Laboratory, California Institute of Technology, 4800 Oak Grove Drive, Pasadena, CA 91109, U.S.A.*

SUMMARY

On-going development of Ka-band capability for the Deep Space Networks (DSN) will radically increase the bandwidth available to support advanced mission concepts envisioned for future robotic as well as human exploration of Mars and beyond. While Ka-band links can operate at much higher data rate than X-band, they are much more susceptible to fluctuating weather conditions and manifest a significant trade-off between throughput and availability. If the operating point is fixed, the maximum average throughput for deep space Ka-band link is achieved at about 80% availability, i.e. weather-related outages will occur about 20% of the time. Low availability increases the complexity of space mission operation, while higher availability would require additional link margins that lowers the overall throughput. To improve this fundamental throughput-availability trade-off, data rate adaptation based on real-time observation of the channel condition is necessary.

In this paper, we model the Ka-band channel using a Markov process to capture the impact of the temporal correlation in weather conditions. We then develop a rate adaptation algorithm to optimize the data rate based on real time feedback on the measured channel conditions. Our algorithm achieves both higher throughput and link availability as compared to the constant rate scheme presently in use.

Received 12 June 2006; Revised 23 August 2006; Accepted 1 September 2006

KEY WORDS: Ka-band; satellite communications; link optimization; rate adaptation

1. INTRODUCTION

Ka-band transmission is viewed as a primary means for meeting the increasing demands for high data rate services of space exploration missions. Due to the increase in antenna gains at higher frequencies, an improvement in the signal strength by a factor of four can be expected in

*Correspondence to: Jun Sun, Massachusetts Institute of Technology, Cambridge, MA 02139, U.S.A.
† E-mail: junsun@mit.edu

Contract/grant sponsor: National Aeronautics and Space Administration; contract/grant number: NAG3-2835

the transition from X-band to Ka-band [1]. Moreover, at Ka-band, deep space communications is allocated 500 MHz of bandwidth compare to the 50 MHz of bandwidth allocated to the X-band [1]; leading to even greater increase in throughput when using Ka-band.

Although the throughput gain in Ka-band can be significant, Ka-band data transmission is susceptible to weather fluctuations. The deep space systems use receivers with very low noise temperatures of approximately 25 K. This makes them extremely sensitive to atmospheric effects [2, 3]. Weather events, such as rain and clouds, increase the moisture in the atmosphere; and consequently the noise temperature.

The proposed data transmission scheme in Ka-band, which is going to be demonstrated on the Mars Reconnaissance Orbiter (MRO), uses constant rate transmission (CRT). Specifically, during a particular communication session, based on the statistics of the atmospheric noise temperature and pass geometry, a link configuration is decided in advance to achieve a constant transmission rate. When the actual transmission takes place, the targeted data rate can be achieved with acceptable reliability if the atmospheric noise temperature is below a certain threshold noise temperature. If the noise temperature exceeds the threshold, significant data corruption and loss of synchronization will occur, making the link unusable.

An immediate consequence of using a pre-determined, fixed rate transmission scheme is the disruption of data continuity due to bad weather. Weather phenomena such as microbursts can significantly increase the system noise temperature thus causing outages for a short period of time [1]. If a timely decision on whether to retransmit the lost data cannot be made, such disruptions will greatly complicate mission operations. In order to ensure the reliability of a communication link, additional power margin will be added to combat the weather fluctuation, at the expense of link throughput.

In this paper we propose to use an adaptive rate transmission (ART) scheme to combat the weather effect associated with the Ka-band link while maintaining data continuity and high throughput. Specifically, our ART scheme predicts the channel conditions (i.e. the atmospheric noise temperature and attenuation) based on the current and past noise temperature observations. A transmission rate is then chosen after adding an appropriate margin to the predicted link budget. This additional power margin is essential to mitigate any prediction errors. The transmitter adapts its transmission rate at regular intervals of relatively short duration (e.g. 5 min). If the predicted noise temperature plus margin is higher than the actual noise temperature during the interval, data can be successfully transmitted at the chosen data rate.

Using atmospheric noise temperature data collected at the Deep Space Network (DSN) Madrid site for 1678 days, we compare the performance of the CRT scheme and the ART scheme in terms of data availability (continuity) and throughput. For the CRT scheme, the maximum throughput is achieved with a temperature threshold of 16 K; which also yields 80% availability. In contrast, as shown in Figure 1 the adaptive rate scheme achieves 40% greater throughput for the same (80%) level of availability. A similar comparison, at different availability levels, is also shown in the figure. For example, at 99% data availability, the throughput of the ART scheme is more than four times that of the CRT scheme. Later in this paper, we also quantify the throughput gain using noise temperature data collected at a rate of one sample per second during the NASA Advanced Communications Technology Satellite (ACTS) propagation experiment. This second-by-second data is useful in the lunar communication scenario since the round-trip signal propagation delay from the earth to the moon is about 3 s. Due to the high correlation among the second-by-second data, the

DOI: 10.1002/sat

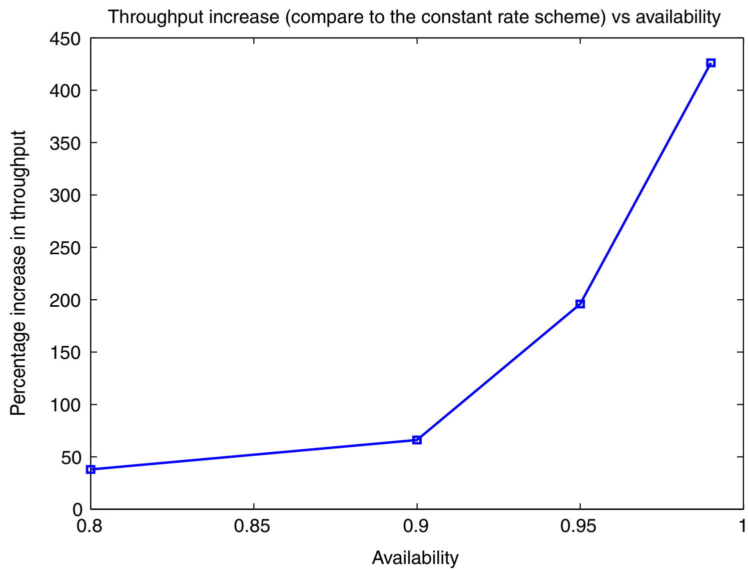

Figure 1. Percentage throughput increase of ART scheme over CRT scheme for different link availabilities.

throughput improvement when using the adaptive transmission scheme is more pronounced than that of the data collected at Madrid.

For clarity of presentation, we have excluded the deterministic variation of spacecraft elevation angle from our analytic model because its impact can be overcome by pre-scheduled adjustments to the transmit power or data rate. These adjustments to deterministic fluctuations can be easily handled by both the ART and CRT schemes. Of course, such adjustments do not take into account the stochastic fluctuations due to weather effects. Hence, the focus of the ART scheme is to adapt the data rate to stochastic fluctuations in the noise temperature.

Using rate adaptation scheme to improve throughput for a satellite link has been investigated by numerous researchers. In [4], Choi and Chan developed a statistical and spectral analysis for signal fading over satellite–earth path where scintillation and rain attenuation are dominant factors. They introduced a continuous power control and discrete rate control strategy, through which they built a set of modulation/code states, and discretely change the modulation symbol size and the code rate from state to state. Significant gain in performance is achieved through the adaptive scheme. In wireless communications, Balachandran *et al.* [5] proposed a technique to measure channel quality in terms of signal-to-interference plus noise ratio (SINR) for the transmission of signals over fading channels. They focused on data rate adaptation and proposed a set of coded modulation schemes which utilize the SINR estimate to adapt between modulations, thus improving data throughput. Their simulation results show that the proposed scheme works well across the entire range of Dopplers to provide near-optimal rate adaptation to average SINR. Prediction model studies for ACTS experiment can be found in [6–10].

The rest of this paper is organized as follows: Section 2 describes the Ka-band link margin and the atmospheric noise measurement data. The details of the CRT scheme and ART scheme

DOI: 10.1002/sat

are presented in Section 3. Section 4 describes the prediction algorithm and the algorithm for choosing the adaptive margin in the ART scheme. Section 5 compares the CRT scheme with the ART scheme in terms of throughput performance and link availability. In Section 6, we discuss the throughput gain when using the second-by-second data collected at the NASA ACTS experiment. Section 7 concludes the paper.

2. LINK MARGIN ANALYSIS

The standard link equation that relates the transmission rate to the required signal-to-noise ratio (SNR) per bit is given by [11]

$$\frac{P_r}{N_0} = R\left(\frac{\mathscr{E}_b}{N_0}\right)_{req} \tag{1}$$

The received SNR on the ground, P_r/N_0, is given by

$$\frac{P_r}{N_0} = P_{Amp} \cdot \varepsilon_{Amp} \cdot \frac{4\pi^2 r_{sc}^2}{\lambda_2} \cdot \varepsilon_{sc} \cdot L_{psc}^{-1} \cdot \left(\frac{\lambda}{d}\right)^2 \cdot L_{Atm}^{-1} \cdot L_{pg}^{-1} \cdot \frac{4\pi^2 r_G^2}{\lambda^2} \cdot \varepsilon_G \cdot (k \cdot T_{sys})^{-1} \tag{2}$$

In the above equation, P_{Amp} is the power into the spacecraft amplifier; ε_{Amp} is the amplifier efficiency; λ is the RF wavelength; r_{sc} and r_G are spacecraft and ground antenna radii, respectively; L_{psc} and L_{pg} are the spacecraft and ground pointing losses, respectively; ε_{sc} and ε_G are the spacecraft and ground antenna efficiencies, respectively; and d is the distance between the spacecraft and the Earth. L_{Atm} is the loss due to atmospheric absorption and scattering; T_{sys} is the ground system noise temperature; and k is Boltzmann's constant [12]. Both L_{Atm} and T_{sys} are related to the atmospheric noise temperature, T_{atm}. Specifically, the atmospheric loss L_{Atm} is related to T_{atm} through the following approximation [12]:

$$L_{Atm} \approx \begin{cases} \dfrac{275}{275 - T_{atm}}, & T_{atm} < 275 \\ \infty & \text{otherwise} \end{cases} \tag{3}$$

The system noise temperature, T_{sys}, reflects how noisy the system is. It consists of equipment and antenna noise temperature, atmospheric noise temperature and observed cosmic background noise. That is

$$T_{sys} = T_{eq} + T_{atm} + \frac{2.7}{L_{Atm}} \tag{4}$$

To illustrate the relationship between weather (i.e. T_{sys}) and the transmission rate, we have

$$R = \frac{\alpha}{T_{eq} + T_{atm} + 2.7/L_{Atm}} \frac{275 - T_{atm}}{275} \Bigg/ \left(\frac{\mathscr{E}_b}{N_0}\right)_{req} \tag{5}$$

where α encapsulates the rest of the terms in Equation (2). For a transmission at rate R to be successful, we must have

$$\frac{\alpha}{T_{eq} + T_{atm} + 2.7/L_{Atm}} \frac{275 - T_{atm}}{275} \Bigg/ R \geqslant \left(\frac{\mathscr{E}_b}{N_0}\right)_{req} \tag{6}$$

In the CRT scheme, a transmission rate and the required SNR per bit are selected first. If the actual SNR per bit at the receiver side is greater than the required SNR per bit, the transmission will be successful. Based on the weather statistics, one can select a rate such that transmissions are successful at a certain percentage of the time. For the CRT scheme, there is a trade-off between the transmission rate and the link availability. Using a higher data rate, requires lower noise temperature; and that occurs with lower probability. Using the ART scheme, the atmospheric noise temperature in the future is predicted first. More specifically, if the current time is t, it is necessary to predict the atmospheric noise temperature at time $t + L$, where L is at least the signal propagation time from the ground to the spacecraft and back (i.e. one round trip time). In the case of the MRO, the round trip time is usually between 20 and 30 min. Given the predicted atmospheric noise temperature and the required SNR, a projected transmission rate can be obtained. A transmission at a certain projected rate is successful only if the actual received SNR is greater than the required SNR. In order for this ART scheme to work properly, it is necessary to combat the prediction error. By adding a margin Δ to the predicted atmospheric noise temperature, one can decrease the probability that the actual received SNR is smaller than the required SNR, hence, assuring higher link availability. As we will see later, the way in which the margin Δ is chosen will have a significant impact on the performance of the adaptive transmission scheme.

The atmospheric noise temperature data used in this paper is measured at Deep Space Communications Complex 60 (Madrid) using a water vapour radiometer (WVR) over 1678 days. The temperature data were gathered at the rate of one measurement every 5 min. Figure 2 shows the cumulative distribution function of T_{atm}. It can be seen from the figure that for 80% of the time the noise temperature is below 16 K; similarly for 85, 90 and 99% availability, the atmospheric noise temperature are below 22, 41.5, and 89.3 K, respectively.

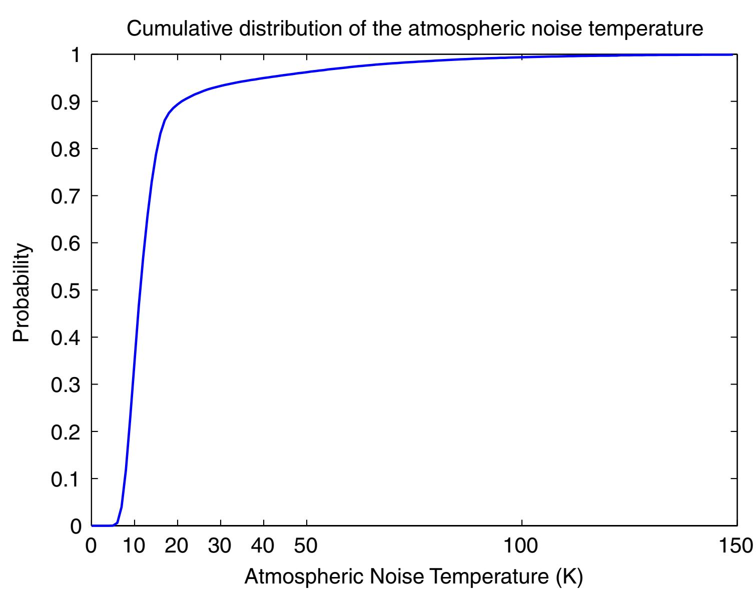

Figure 2. The cumulative distribution function of T_{atm}.

DOI: 10.1002/sat

3. THROUGHPUT AND LINK AVAILABILITY

To get estimate of the throughput performance of the CRT scheme using the measured noise temperature data, we first calibrate our link model with a baseline design by selecting a threshold atmospheric noise temperature T_0 and the required SNR per bit for link availability. Hence the transmission rate at the noise temperature threshold, $R_c(T_0)$, is given by

$$R_c(T_0) = \frac{\alpha}{T_{eq} + T_0 + 2.7/L_{Atm}} \frac{275 - T_0}{275} \bigg/ \left(\frac{\mathscr{E}_b}{N_0}\right)_{req} \tag{7}$$

Let N denote the total number of data measurements and $T(i)$ denote the ith atmospheric noise temperature measurement. The average transmission rate $\bar{R}_c$ with a threshold temperature T_0 can be written as follows:

$$\bar{R}_c(T_0) = \frac{1}{N}\sum_{i=1}^{N} R_c(T_0) \cdot \mathbf{1}_{T(i)<T_0} \tag{8}$$

where

$$\mathbf{1}_{T(i)<T_0} = \begin{cases} 1 & \text{if } T(i) < T_0 \\ 0 & \text{otherwise} \end{cases} \tag{9}$$

The other performance metric that we are interested is link availability, denoted here as $A(T_0)$, and is given by

$$A(T_0) = \frac{1}{N}\sum_{i=1}^{N} \mathbf{1}_{T(i)<T_0} \tag{10}$$

In general the average transmission rate is a concave function of the reference temperature T_0. When T_0 is low, the average data rate is low due to frequent outages. However, if T_0 is high, the link availability increases but the required SNR per bit forces low data rate transmission. So it is clear for a fixed rate scheme, there is a trade-off between availability and throughput. From the atmospheric noise temperature data, the maximum $\bar{R}_c$ is achieved when $T_0 = 16$ K. The link availability, given $T_0 = 16$ K, is about 80%. For 20% of the time, the link will not be available for reliable communications. Moreover, since the time scale for weather event is typically long (e.g. minutes to hours); the outage period presents a significant operational challenge to missions that desire constant monitoring/control of remote spacecrafts.

Using an ART scheme, intuitively, the trade-off between throughput and availability can be eliminated to a great extent. By setting a new threshold for each time interval (5-min interval is used in this paper), the adaptive scheme can have both good throughput when channel quality is good and good availability performance when the weather condition is poor. Specifically, at time t, the ART scheme predicts the atmospheric noise temperature at time $t + t_0$, denoted as $T_p(t + t_0)$, where t_0 is at least one round trip time from the ground to the spacecraft. To mitigate the effect of the prediction error, a small margin Δ is also added to $T_p(t + t_0)$. Based on $\hat{T}(t + t_0) = T_p(t + t_0) + \Delta$, the projected rate of transmission at time $t + t_0$, denoted as $R_p(t + t_0)$, is obtained as follows:

$$R_p(t + t_0) = \frac{\alpha}{g(\hat{T}(t + t_0))} \bigg/ \left(\frac{\mathscr{E}_b}{N_0}\right)_{req} \tag{11}$$

where

$$g(x) = \left(T_{\text{eq}} + x + 2.7 \cdot \frac{275 - x}{275}\right) \cdot \frac{275}{275 - x} \tag{12}$$

When the actual transmitted signal reaches the ground receiver at time $t + t_0$, the actual SNR per bit is given by

$$\text{SNR}(t + t_0) = \frac{\alpha / g(T(t + t_0))}{R_{\text{p}}(t + t_0)} \tag{13}$$

$$= \frac{g(\hat{T}(t + t_0))}{g(T(t + t_0))} \cdot \left(\frac{\mathscr{E}_{\text{b}}}{N_0}\right)_{\text{req}} \tag{14}$$

If $\text{SNR}(t + t_0)$ is greater than $(\mathscr{E}_{\text{b}}/N_0)_{\text{req}}$, the transmission is successful. The average throughput of the ART scheme can be written as

$$\bar{R}_{\text{a}} = \frac{1}{N - t_0} \sum_{t=1}^{N-t_0} R_{\text{p}}(t + t_0) \cdot \mathbf{1}_{\{\text{SNR}(t+t_0) > (\mathscr{E}_{\text{b}}/N_0)_{\text{req}}\}} \tag{15}$$

Similarly, the availability of transmissions using the ART scheme, denoted here as $A_{\text{a}}(T_0)$, is given by

$$A_{\text{a}} = \frac{1}{N - t_0} \sum_{t=1}^{N-t_0} \mathbf{1}_{\{\text{SNR}(t+t_0) > (\mathscr{E}_{\text{b}}/N_0)_{\text{req}}\}} \tag{16}$$

4. ADAPTIVE RATE TRANSMISSION SCHEME: PREDICTION AND MARGIN

4.1. *Atmospheric noise temperature prediction*

To predict the atmospheric noise temperature one round trip time ahead into the future, we first investigate the correlations between the atmospheric noise temperature measurements. Figure 3 plots the autocorrelation function of the noise samples. The correlation between samples decreases as the time between samples increases. Now consider a first order autoregressive process described by the following equation:

$$y(t) = a_1 \cdot y(t - 1) + w(t) \tag{17}$$

where $y(t)$ denotes the atmospheric noise temperature measurement at time t, a_1 is a constant, and $w(t)$ denotes the random fluctuation of the temperature at time t independent of $w(s)$ for all $s < t$. Its autocorrelation function is defined as

$$R(k) = E[y(t) \cdot y(t - k)]$$

From Equation (17), a recursive form of the autocorrelation function can be written as the following:

$$R(k) = a_1 \cdot R(k - 1), \quad k > 0 \tag{18}$$

Solving the above equation, we have

$$R(k) = a_1^k, \quad k \geqslant 0$$

DOI: 10.1002/sat

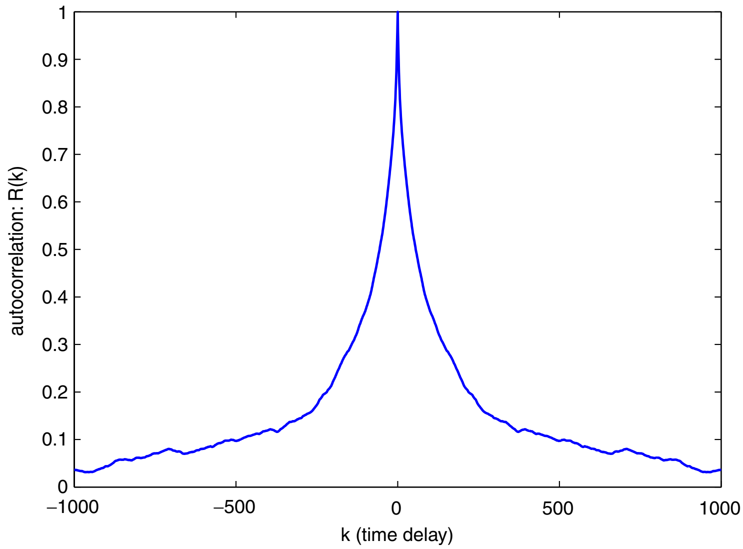

Figure 3. The autocorrelation function of the atmospheric noise temperature data with sampling interval of 5 min.

From Figure 3, we see that the empirical autocorrelation function fits the first order autocorrelation model very well. Examining the autocorrelation function for $k \geqslant 0$, as k increases, $R(k)$ decreases exponentially for $a_1 < 1$. Hence, Equation (17) can be used to describe the atmospheric noise temperature measurements. Now, to predict the atmospheric noise temperature l samples ahead, we only need to look at the most recent sample since the process is a first order autoregressive process or a Markov process. Let $\hat{y}(t+l)$ be the predicted noise temperature at time $t+l$. we can write

$$\hat{y}(t+l) = c \cdot y(t) \tag{19}$$

To minimize the prediction mean square error, we have

$$E[(\hat{y}(t+l) - y(t+l))y(t)] = 0$$

Solving for the coefficient c, we have

$$c = \frac{R(l)}{R(0)}$$

4.2. Margin in the adaptive rate transmission scheme

We first investigate the performance of the ART scheme when a constant margin is added to the predicted atmospheric noise temperature. The result is presented in Figure 4. The throughput of the adaptive transmission scheme with constant margin is compared with the maximum throughput of the CRT scheme. The service availability is defined as the fraction of the 5 min intervals that the transmissions are successful. Note that to achieve the maximum throughput in the constant rate scheme results in a service availability of 80%. In comparison, the ART

DOI: 10.1002/sat

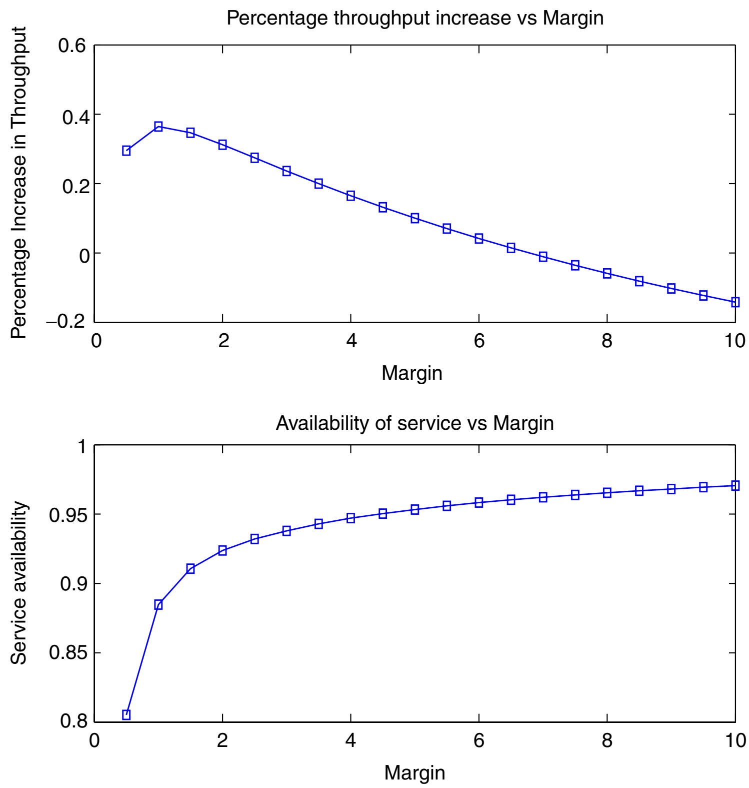

Figure 4. The percentage throughput increase (as compared to the CRT scheme) and availability in the adaptive rate transmission scheme with a constant margin.

scheme achieves both a higher throughput and a higher availability than the CRT scheme; even with the constant margin as shown in Figure 4.

In Figure 4, we see an improvement in the trade-off between the throughput and the service availability using the ART scheme. As the margin increases, the throughput decreases and availability increases. Since the sole purpose of adding a margin to predict atmospheric noise temperature is to mitigate the prediction error, knowing how good the prediction is can be very useful in determining the right margin levels. That is, if the prediction is good, it is unnecessary to add a large margin.

Intuitively, if the past atmospheric temperature measurements have little fluctuation, we know the prediction should be good. Also, if the current atmospheric temperature is low (i.e. the weather is good), the predicted temperature in the future is usually more accurate because the atmospheric condition under good weather is less variable compared to poor weather say when a storm system is present. Hence, to estimate the accuracy of the prediction, our ART scheme will take the following two factors into consideration: the standard deviation of the past atmospheric noise measurement and the current atmospheric noise temperature. To get the standard deviation of the past M measurements, say $\{T(-M+1), T(-M+2), \ldots, T(0)\}$, we

DOI: 10.1002/sat

use the following:

$$\mathrm{SD}(0) = \sqrt{\frac{1}{M}\sum\nolimits_{i=1}^{M}[T(-M+i)-\bar{T}(0)]^2} \tag{20}$$

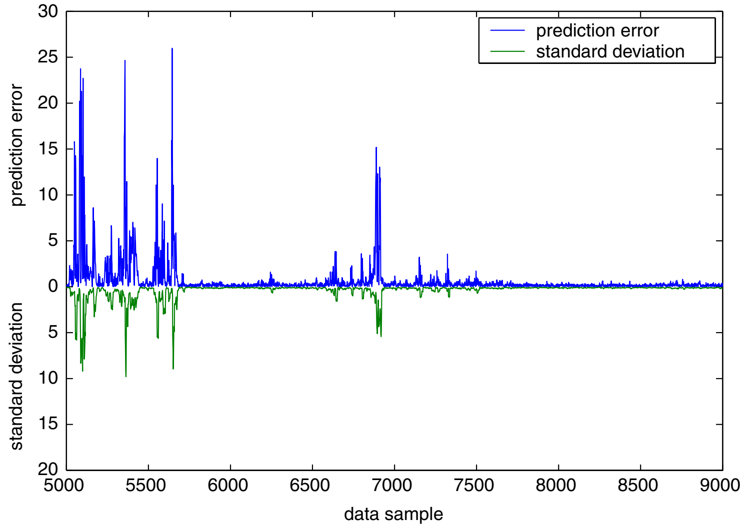

Figure 5. The correlation between the standard deviation of past measurements and the prediction error.

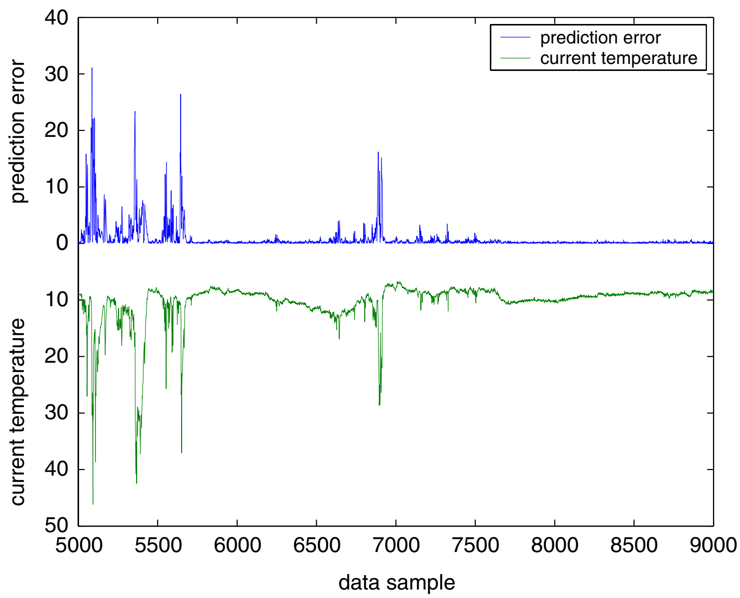

Figure 6. The correlation between the current measurements and the prediction error.

DOI: 10.1002/sat

where

$$\bar{T}(0) = \frac{1}{M}\sum_{i=1}^{M} T(-M+i)$$

Figure 5 shows how the prediction error and the standard deviation of past measurements are related for data samples 5000 to 9000. We can see that the prediction error is large whenever the standard deviation of the past measurements is large. Figure 6 shows the prediction error and the current atmospheric noise temperature. Low atmospheric noise temperature normally associates with small prediction error. Based on these two observations, the margin for each 5-min interval is chosen adaptively as follows:

$$\Delta(t) = c_1 \cdot \mathrm{SD}(t) + c_2 \cdot T(t) \tag{21}$$

where c_1 and c_2 are constants that can be chosen to achieve a trade-off between throughput and availability.

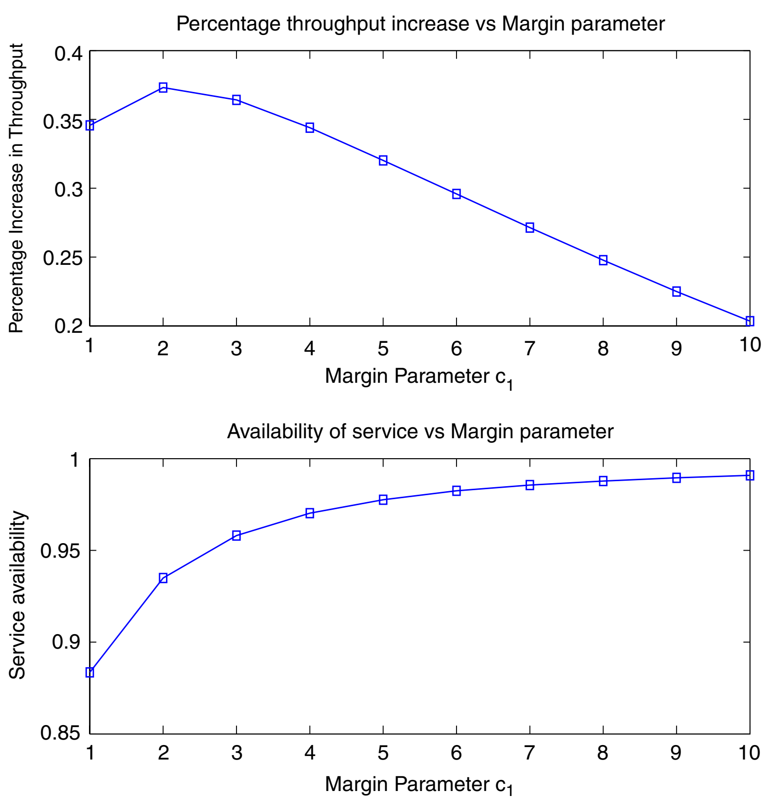

Figure 7. The percentage throughput increase and availability in the adaptive rate transmission scheme with an adaptive margin.

DOI: 10.1002/sat

5. COMPARISON: THROUGHPUT AND SERVICE AVAILABILITY

Figure 7 shows the performances of the transmission scheme that implements the adaptive margin described in Equation (21). In this plot, we show how the throughput (compared to that of the CRT scheme with 80% weather availability) and availability changes when c_1 increases. With $c_1 = 2$, the throughput of the adaptive transmission scheme is 37% more than the maximum achievable throughput of the CRT scheme; the service availability is 94%, compared to the 80% availability of the CRT scheme. At $c_1 = 10$, the throughput of the adaptive transmission scheme is still 20% more than the maximum throughput of the CRT scheme while the availability increases to 99%. Thus, the ART scheme not only provides significant throughput gain but also greatly increases the data availability.

To make a fair comparison, Figure 1 plots the throughput increase in using the adaptive scheme with respect to the CRT schemes, for achieving 99, 95, 90 and 80% service availability. As we can see from this figure, for the CRT to achieve 99% service availability, the resulting throughput is only about $\frac{1}{4}$ of that of the ART scheme.

As mentioned previously, an important advantage of using the ART scheme is to provide data continuity. Using the CRT scheme, data will be lost whenever the atmospheric noise temperature is above the threshold temperature, resulting in a complicated retransmission process and mission operational procedure to work around the outage. Figure 8 presents a histogram of the outage durations using the two different transmission schemes. From the figure, we see that outages occur much more frequently and with longer duration when using the CRT scheme.

In all the previous throughput results, we assume that the equivalent noise temperature of the ground equipment, T_{eq}, is zero. In Figure 9, we investigate the effect of the throughput performance when the equipment noise is between 0 and 25 K. For achieving 95% weather availability, the throughput increase in the ART scheme with respect to the CRT scheme decreases from 200 to 60% as the equipment noise increases from 0 to 25 K.

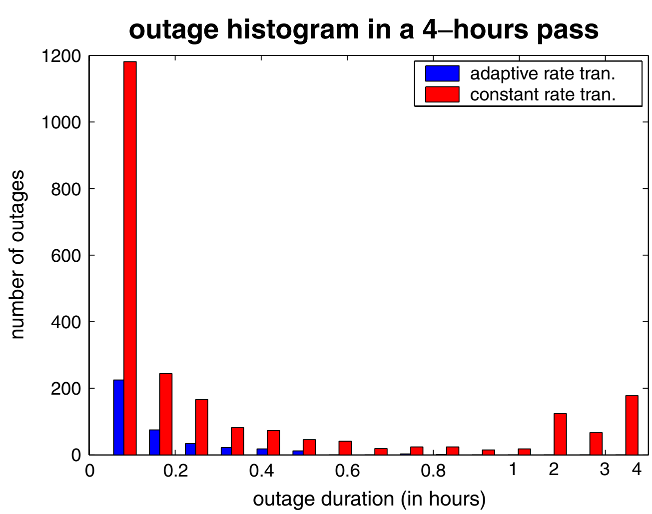

Figure 8. Histogram of outage duration for both the ART and CRT schemes.

DOI: 10.1002/sat

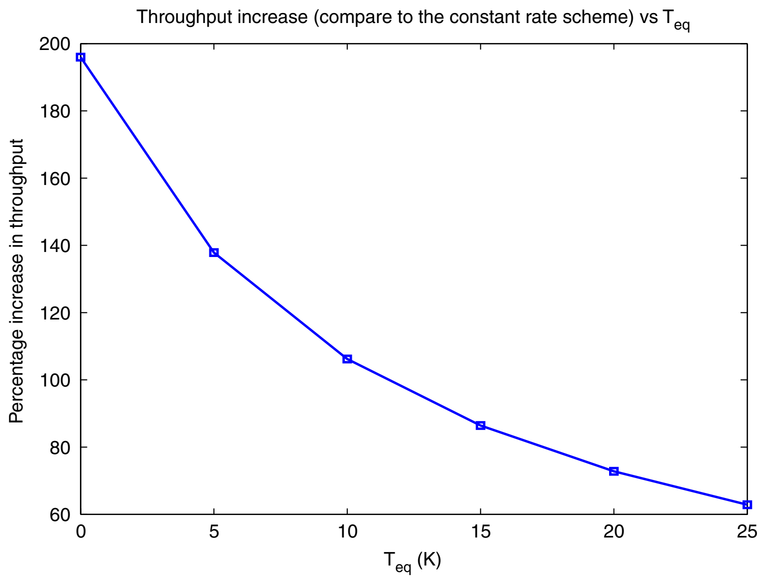

Figure 9. The effect of equipment noise on the throughput increase.

6. NASA ACTS Ka-BAND EXPERIMENT

The NASA ACTS propagation experiment was designed to obtain slant-path beacon attenuation statistics at Ka-band frequencies [13, 14]. ACTS carries beacons at 20.2 and 27.5 GHz for use in the maintenance and control of the ACTS communications networks. In contrast to the DSN, the earth terminal's receiver of the ACTS experiment employ low-noise systems with noise temperatures of about 150 K, compared to deep space systems which employ receivers with much lower noise temperatures of approximately 25 K. The second-by-second daily attenuation time series of the beacons are used in this section. This second-by-second attenuation data is going to be useful for lunar communications because the round-trip propagation delay from the earth to the moon is about 3 s. The availability of the signal attenuation data at the seconds level enables us to evaluate the throughput gain using the ART in a lunar–earth communication scenario. In this paper, we will focus on the attenuation data for beacons at 27.5 GHz. For consistency with the analysis in the previous part, we first convert the attenuation of signal in atmosphere (i.e. $L_{\rm atm}$) to the atmospheric noise temperature (i.e. $T_{\rm atm}$) through the following equation:

$$L_{\rm Atm} \approx \begin{cases} \dfrac{275}{275 - T_{\rm atm}}, & T_{\rm atm} < 275 \\ \infty & \text{otherwise} \end{cases} \tag{22}$$

The total system noise temperature, as we mentioned before, consists of the equipment noise temperature and the atmospheric noise temperature. Since the equipment noise temperature depends on specific receiver, we will simply represent it as a variable $T_{\rm eq}$. In this paper, we are

DOI: 10.1002/sat

mainly interested in the effect of the atmospheric noise on the communication link and how to combat it using ART schemes.

In this section, we used the attenuation data of the beacon at 27.5 GHz which was collected at Norman, OK in 1995. The data were gathered at a rate of one measurement per second. Figure 10 shows the cumulative distribution function of T_{atm}. It can be seen from the figure that for 85% of the time the noise temperature is below 46.2 K; similarly for 90, 95 and 99% availability, the atmospheric noise temperature are below 52.4, 68.7 and 100 K. Compared to the cdf of the atmospheric noise temperature in Figure 2, the atmospheric noise temperature data collected in the ACTS experiment is significantly higher than the atmospheric noise temperature collected using the WVR at Madrid. To see correlations among samples, we plot the following two figures. In Figure 11, we plot the correlation of data gathered at a rate of one measurement per second. For this data which are gathered at a rate of one measurement per second, we then take a data sample out of every 300 data samples to form a new data set (corresponding to one measurement every 5 min). The correlation of this new data set is then plotted in Figure 12.

For the data set with one sample per second, we see that there is a significant correlation among samples even when the lag k is big. However, for the data set with one sample every 5 min, the correlation decreases rapidly for small value of k and approaches a constant as the k gets larger. Comparing both figures with the data collected at the DSN, we find that the correlation of the ACTS data is more significant.

We then compare the performance of the CRT scheme and the ART scheme in terms of data availability (continuity) and throughput. Since we are mainly considering the lunar communication scenario, we want to predict the atmospheric noise temperature 3 s ahead based on the current and past noise temperature measurement. The margin in the ART scheme

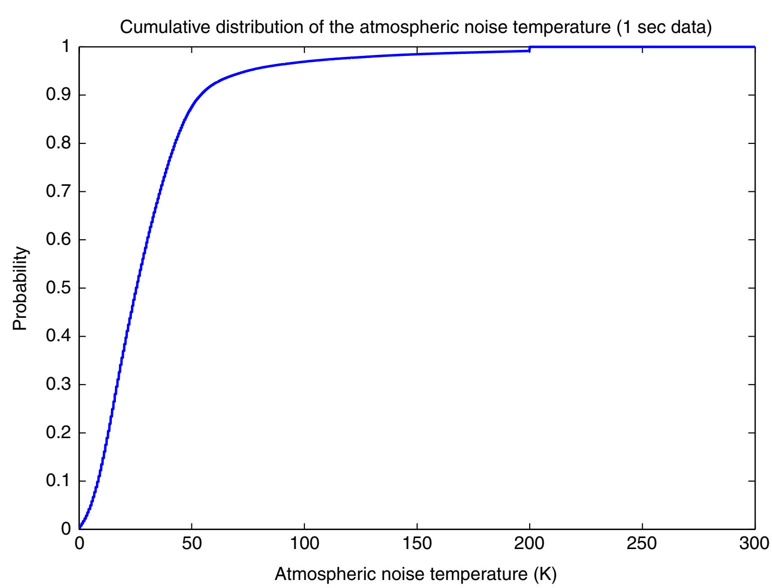

Figure 10. The cumulative distribution function of T_{atm} at Norman, OK (ACTS experiment).

DOI: 10.1002/sat

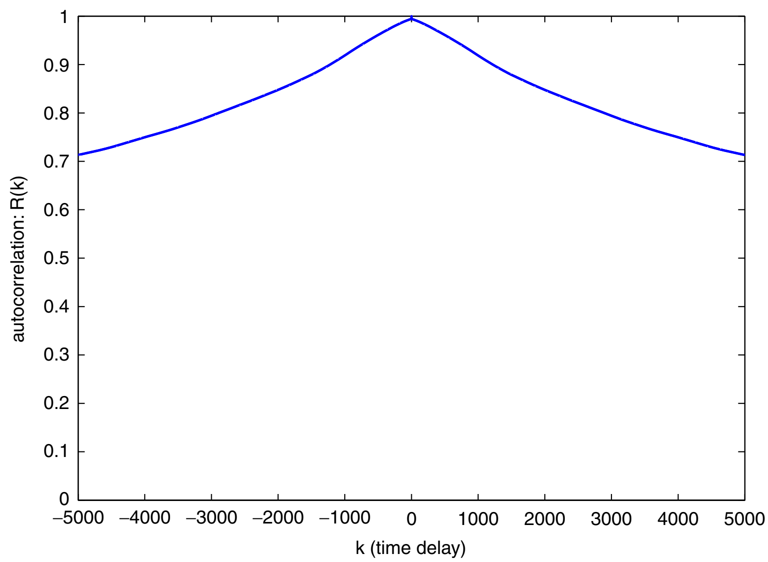

Figure 11. The autocorrelation function of the atmospheric noise temperature data with sampling interval of 1 s.

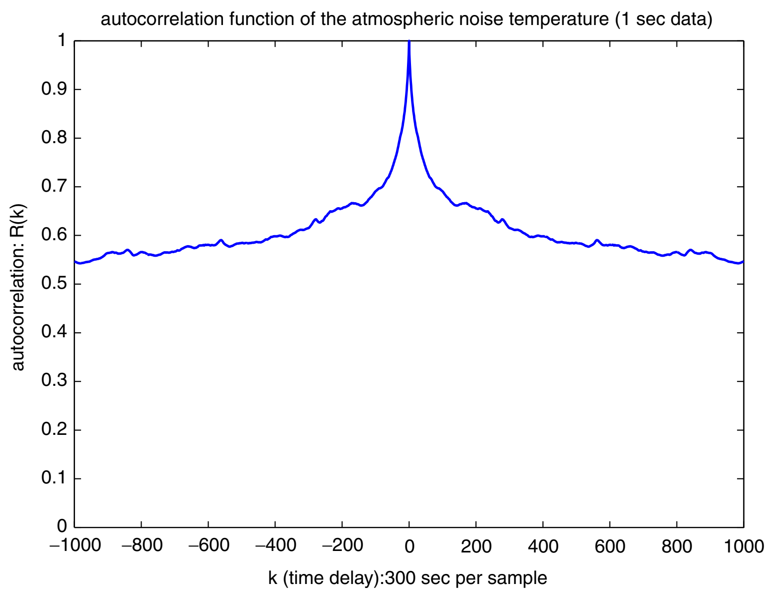

Figure 12. The autocorrelation function of the atmospheric noise temperature data with sampling interval of 5 min.

is chosen according to Equation (21). In this lunar communication scenario, the parameter c_1 is chosen to be equal to 2, and c_2 is chosen to be 0.05. Due to the high correlation among the data with 1 s sampling rate, the prediction performance is significantly better than that of the DSN

DOI: 10.1002/sat

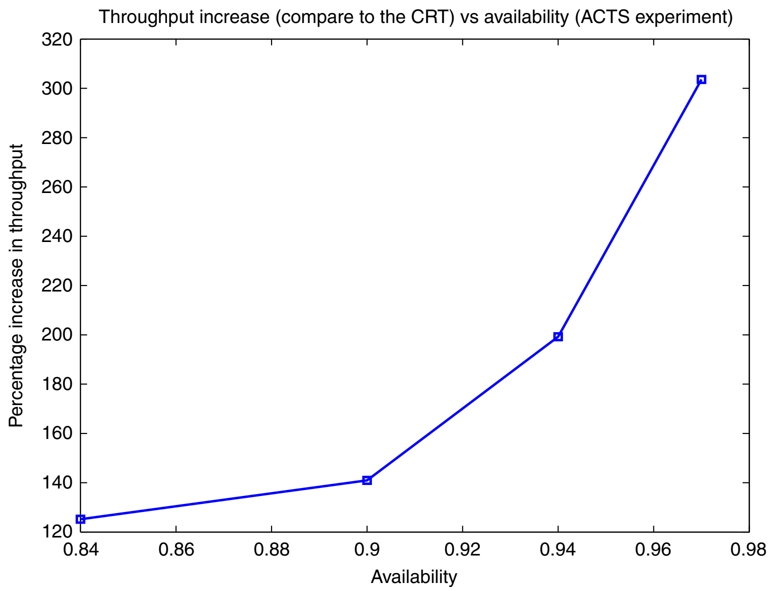

Figure 13. Percentage throughput increase of ART scheme over CRT scheme for different link availabilities.

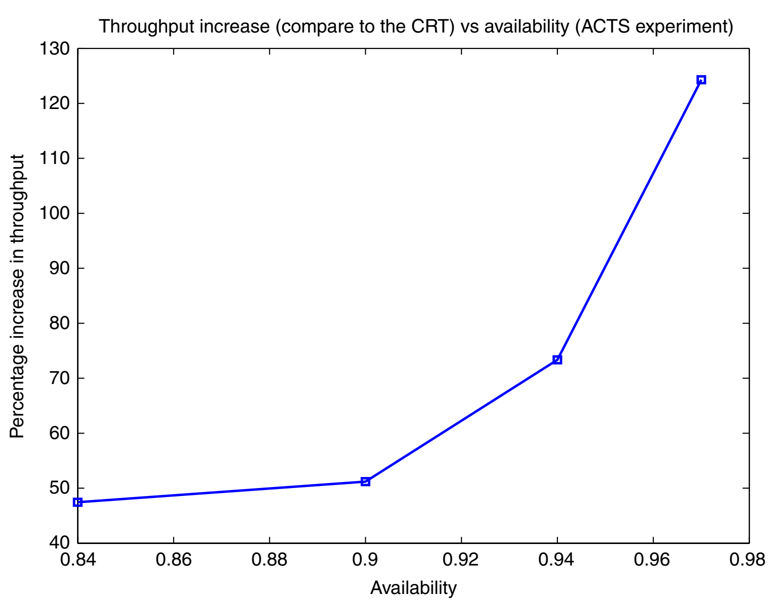

Figure 14. Percentage throughput increase of ART scheme over CRT scheme for different link availabilities with $T_{eq} = 25$ K.

data. The performance improvement of the adaptive scheme over the constant rate scheme is presented in Figure 13. In Figure 13, the equipment noise T_{eq} was set to be zero. The throughput improvement for the case that $T_{eq} = 25$ K is presented in the Figure 14.

7. CONCLUSION

In this paper, we propose a rate adaptive transmission scheme to mitigate weather effects associated with the Ka-band link while maintaining data continuity and high throughput. During a fixed interval of consideration, the ART scheme predicts the atmospheric noise temperature at least one round trip time ahead. The adverse effect of prediction error on the success of the transmission is reduced by dynamically adjusting the link margin.

Our adaptive scheme leads to both a significant throughput increase and a dramatic increase in link availability. For example, when operating at 99% availability, our adaptive algorithm achieves a throughput increase of 400% as compared to the CRT scheme at the same level of link availability. The gain in throughput is more significant when using the second-by-second data collected in the ACTS experiment. For 85% of transmission availability, the throughput gain when using the adaptive scheme is more than twice of the throughput of the CRT scheme. The usage of ART will be critical to the future of space science and exploration activities where high data rate and high availability communication are essential for ensuring mission safety and success.

ACKNOWLEDGEMENTS

This research was partially carried out at the Jet Propulsion Laboratory, California Institute of Technology, under a contract with the National Aeronautics and Space Administration, and at MIT, under NASA Space Communication Project grant number NAG3-2835.

REFERENCES

1. Townes SA, Amoozegar F, Border JS, Breidenthal JC, Morabito D, Moyd KI, Patterson JE, Shambayati S. Operational demonstration of Ka-band telecommunications for the Mars reconnaissance orbiter. *IEEE Aerospace Conference 2003*, Big Sky, Montana, March 2003.
2. Davarian F, Shambayati S, Slobin S. Deep space Ka-band link management and Mars reconnaissance orbiter: long-term weather statistics versus forecasting. *Proceedings of the IEEE* 2004; **92**(12):1879–1894.
3. Shambayati S. On the benefits of short-term weather forecasting for Ka-band (32 GHz). *IEEE Aerospace Conference*, Big Sky, Montana, 7–12 March 2004.
4. Choi JP, Chan VWS. Prediction and adaptation of satellite channels with weather-induced impairments. *IEEE Aerospace Conference*, Big Sky, Montana, vol. 3, 2002; 3/1209–3/1219.
5. Balachandran K, Kadaba SR, Nanda S. Channel quality estimation and rate adaptation for cellular mobile radio. *IEEE Journal on Selected Areas in Communications* 1999; **17**(7):1244–1256.
6. Crane RK, Robinson PC. ACTS propagation experiment: rain-rate distribution observations and prediction model comparisons. *Proceedings of the IEEE* 1997; **85**(6):946–958.
7. Crane RK, Dissanayake AW. ACTS propagation experiment: attenuation distribution observations and prediction model comparisons. *Proceedings of the IEEE* 1997; **85**(6):879–892.
8. Bauer R. Ka-band propagation measurements: an opportunity with the advanced communications technology satellite (ACTS). *Proceedings of the IEEE* 1997; **85**(6):853–862.

9. Goldhirsh J, Musiani BH, Vogel WJ. Cumulative fade distributions and frequency scaling techniques at 20 GHz from the advanced communications technology satellite and at 12 GHz from the digital satellite system. *Proceedings of the IEEE* 1997; **85**(6):910–916.
10. Alouini M, Borgsmiller SA, Steffes PG. Channel characterization and modeling for Ka-band very small aperture terminals. *Proceedings of the IEEE* 1997; **85**(6):981–997.
11. Proakis JG. *Digital Communications* (3rd edn). McGraw-Hill: New York, 316–319.
12. Shambayati S. On the use of W-band for deep space communications. *IPN Progress Report 42-154*, August 2003.
13. Crane RK, Wang X, Westenhaver DB, Vogel WJ. ACTS propagation experiment: experiment design, calibration, and data preparation and archival. *Proceedings of the IEEE* 1997; **85**(6):863–878.
14. Mayer CE, Jaeger BE, Crane RK, Wang X. Ka-band scintillations: measurements and model predictions. *Proceedings of the IEEE* 1997; **85**(6):936–945.

AUTHORS' BIOGRAPHIES

Jun Sun received his BS degree in Computer Engineering from University of Florida in 1997 and his MS in Electrical Engineering from Massachusetts Institute of Technology in 2002. He is currently a PhD student in the Laboratory for Information and Decision Systems at MIT. His research interest is on communication networks with emphasis on satellite and wireless networks.

Jay Gao joined the Jet Propulsion Laboratory in 2001 and is currently a member of the technical staff in the Communications Networks Group in the Telecommunication Research and Architecture section. His research is primarily focused on space-based wireless communications and networking, with emphasis on applications for the Mars Network. He is currently conducting research for developing quality-of-service (QoS)-aware protocols for the envisioned Interplanetary Network (IPN) and study optimization and protocols for deep space Ka-band communications. He also supports requirements definition and interface design activities for the Department of Defense's Transformational Communications MilSatcom project and system engineering effort for NASA's Exploration System and Mission Directorate (ESMD). Other research interests include optical-based sensor-web, discrete event simulation of distributed communication/sensor systems, energy efficient routing and self-organization algorithm for cooperative signal processing and sensor networks. He received his BS, MS, and PhD degree in Electrical Engineering from UCLA in 1993, 1995, and 2000, respectively.

Shervin Shambayati obtained his Bachelors of Science degree in Applied Mathematics and Engineering in 1989 from California State University, Northridge. Subsequently, he obtained his MSEE, Engineer's Degree and PhD from University of California, Los Angeles in 1991, 1993 and 2002, respectively. In 1993, Dr Shambayati joined the Deep Space Communications Systems Group at Jet Propulsion Laboratory where he took part in development and testing of Deep Space Network's Galileo Telemetry receiver (DGT). In 1997, Dr Shambayati joined the Information Processing Group at JPL where he has been working ever since. With that group Dr Shambayati has been involved in various projects including Mars Global Surveyor's Ka-Band Link Experiment II, Deep Space 1 Ka-band testing and 70 m antenna Ka-band Task. Currently, Dr Shambayati is the Principal Investigator for the Mars Reconnaissance Orbiter Ka-band Demonstration. His current research interests and

DOI: 10.1002/sat

activities include evaluating the effects of weather outages on the spacecraft resources, Ka-band weather forecasting, Ka-band link design and engineering support for implementation of Ka-band services in NASA's Deep Space Network.

Eytan Modiano received his BS degree in Electrical Engineering and Computer Science from the University of Connecticut at Storrs in 1986 and his MS and PhD degrees, both in Electrical Engineering, from the University of Maryland, College Park, MD, in 1989 and 1992, respectively. He was a Naval Research Laboratory Fellow between 1987 and 1992 and a National Research Council Post Doctoral Fellow during 1992–1993. Between 1993 and 1999 he was with MIT Lincoln Laboratory where he was the project leader for MIT Lincoln Laboratory's Next Generation Internet (NGI) project. Since 1999 he has been an Associate Professor in the Department of Aeronautics and Astronautics at MIT. His research is on communication networks and protocols with emphasis on satellite, wireless, and optical networks. He is currently an Associate Editor for Communication Networks for IEEE Transactions on Information Theory and for The International Journal of Satellite Communications. He had served as a guest editor for IEEE JSAC special issue on WDM network architectures; the Computer Networks Journal special issue on Broadband Internet Access; the Journal of Communications and Networks special issue on Wireless *Ad-Hoc* Networks; and for IEEE Journal of Lightwave Technology special issue on Optical Networks. He is the Technical Program co-chair for Wiopt 2006 and Infocom 2007.